

Climate model simulated changes in temperature extremes due to land cover change

F. B. Avila,¹ A. J. Pitman,¹ M. G. Donat,¹ L. V. Alexander,¹ and G. Abramowitz¹

Received 8 June 2011; revised 9 October 2011; accepted 28 December 2011; published 25 February 2012.

[1] A climate model, coupled to a sophisticated land surface scheme, is used to explore the impact of land use induced land cover change (LULCC) on climate extremes indices recommended by the Expert Team on Climate Change Detection and Indices (ETCCDI). The impact from LULCC is contrasted with the impact of doubling atmospheric carbon dioxide (CO₂). Many of the extremes indices related to temperature are affected by LULCC and the resulting changes are locally and field significant. Some indices are systematically affected by LULCC in the same direction as increasing CO₂ while for others LULCC opposes the impact of increasing CO₂. We suggest that assumptions that anthropogenically induced changes in temperature extremes can be approximated just by increasing greenhouse gases are flawed, as LULCC may regionally mask or amplify the impact of increasing CO₂ on climate extremes. In some regions, the scale of the LULCC forcing is of a magnitude similar to the impact of CO₂ alone. We conclude that our results complicate detection and attribution studies, but also offer a way forward to a clearer and an even more robust attribution of the impact of increasing CO₂ at regional scales.

Citation: Avila, F. B., A. J. Pitman, M. G. Donat, L. V. Alexander, and G. Abramowitz (2012), Climate model simulated changes in temperature extremes due to land cover change, *J. Geophys. Res.*, 117, D04108, doi:10.1029/2011JD016382.

1. Introduction

[2] Among the human activities that can impact the climate system, land use induced land cover change (LULCC) is one of the more controversial. There are multiple types of LULCC including deforestation, afforestation, irrigation and urbanization. These have different impacts on net radiation at the land surface [Forster *et al.*, 2007] and its partitioning into sensible and latent heat fluxes [Bala *et al.*, 2007; Pitman *et al.*, 2009]. While afforestation will serve as a carbon sink [e.g., House *et al.*, 2002; Canadell and Raupach, 2008], at least on decadal time scales, some studies suggest that such conversion can increase regional-scale surface warming by reducing the snow-albedo feedback [Betts, 2000]. Unlike greenhouse gases that affect the global climate by warming [Solomon *et al.*, 2007], the directional impact of LULCC on temperature varies between regions and between seasons [de Noblet-Ducoudré *et al.*, 2012]. LULCC typically warms the tropics and cools the midlatitudes [Lawrence and Chase, 2010]. This difference in the sign of the impact of regional LULCC results in negligible changes in key climate variables such as temperature and rainfall when averaged globally [Feddema *et al.*, 2005; Pielke *et al.*, 2011]. At regional scales, however, in regions subjected to significant LULCC, the impact of landscape change on temperature and some hydrometeorological variables can be similar in magnitude

to a doubling of atmospheric CO₂ [Zhao and Pitman, 2002] or other large-scale changes in forcing such as the El Niño-Southern Oscillation [Findell *et al.*, 2009]. A detailed examination of the observational and model-based evidence linking LULCC to local, regional and global scale climate has recently been provided by Pielke *et al.* [2011].

[3] LULCC can affect the regional-scale climate by changing the terrestrial energy and water balance [de Noblet-Ducoudré *et al.*, 2012]. Historic LULCC, largely characterized by deforestation, tends to increase the surface albedo resulting in cooling. However, forest removal also decreases evapotranspiration efficiency and surface aerodynamic roughness, which tends to cause warming by suppressing turbulent energy fluxes [Pielke *et al.*, 2011]. The albedo effect tends to dominate over the midlatitudes, commonly because of increases in snow covered surfaces, while the role of evapotranspiration and aerodynamic roughness length tends to dominate over the tropics [Davin and de Noblet-Ducoudré, 2010].

[4] Previous modeling studies on the impact of LULCC on the climate system have mainly focused on changes in the mean climate. Indeed, there is a significant body of literature demonstrating that LULCC affects the Earth's climate over regions where it occurs [e.g., Bonan, 2008; Findell *et al.*, 2007; Pitman *et al.*, 2009; Pielke *et al.*, 2011] and perhaps even remotely via teleconnections [Hasler *et al.*, 2009; Snyder, 2010; Medvigy *et al.*, 2011]. However, while studying changes in the climatological mean is important, changes in extreme events are likely to have a bigger direct impact on society than changes in the mean [Easterling *et al.*, 2000; Luber and McGeehin, 2008]. This has obvious importance in a stationary climate but becomes even more pressing under

¹Climate Change Research Centre, University of New South Wales, Sydney, New South Wales, Australia.

climate change due to potentially enhanced changes in extremes compared to the mean [Katz and Brown, 1992; Schaeffer et al., 2005].

[5] Temperature extremes are known to be changing globally. Since the middle of the 20th century there has been a positive (warming) shift in the distribution of daily minimum temperature throughout the globe [Caesar et al., 2006], manifested by a significant increase in the number of warm nights globally [Alexander et al., 2006]. A positive shift in the distribution of daily maximum temperature has also been observed, although somewhat smaller than the increase in daily minimum temperature, resulting in a reduction in the diurnal temperature range [Vose et al., 2005]. Recent detection and attribution studies for a range of temperature extremes indicate that human-induced changes in greenhouse gases are factors in these globally observed changes [e.g., Kiktev et al., 2003, 2007; Christidis et al., 2005, 2011]. Global climate projections also indicate that the magnitude of these changes will likely scale with the strength of the emissions scenario [Tebaldi et al., 2006] leading to, for example, more intense, more frequent and longer lasting heat waves in a future warmer climate [Meehl and Tebaldi, 2004].

[6] LULCC can also affect extremes. Irrigation, for example, provides a supply of moisture that enables evaporative cooling to suppress high temperature extremes and may affect low temperature extremes [Pielke et al., 2011, and references therein]. Most recently, Teuling et al. [2010] highlighted how forest and grassland regions of Europe responded differently in terms of heat waves, identifying resilience in deeply rooted forests compared to grasslands. Once linked with the impact of LULCC on land-atmosphere coupling [Seneviratne et al., 2006, 2010] and the recognition that the surface energy balance is strongly affected by the nature of the land cover [Pitman, 2003; Bonan, 2008; Levis, 2010] it is implausible to think that LULCC would not affect temperature extremes provided it is of a sufficient scale and intensity.

[7] However, little is known about the relative magnitude of impacts of LULCC on temperature extremes globally compared to changes due to increases in greenhouse gases. Therefore this paper focuses on a model-based global-scale assessment of how LULCC affects temperature extremes in comparison to the changes caused by increased greenhouse gas concentrations. We explore how some temperature-related extremes are affected by LULCC using a climate model that is coupled to a state of the art land surface scheme that couples the exchange of energy, water and carbon within the canopy. We contrast the impact of LULCC on the temperature extremes indices with that of doubling CO_2 , noting that our $2 \times \text{CO}_2$ simulations are only approximate estimates given they are equilibrium (not transitory) simulations. Our aim is a first order estimate of those extremes indices that are likely affected by LULCC at a scale that is worthy of consideration in future climate change assessments.

2. Methodology

2.1. Climate and Land Surface Model

[8] To simulate the effects of LULCC and changes in atmospheric CO_2 concentrations on the climate, we use CSIRO Mk3L, a global circulation model [Phipps et al.,

2011], coupled with the Community Atmosphere Biosphere Land Exchange model (CABLE) [Wang et al., 2011].

[9] Most of the extremes explored in this paper are intimately associated with how the land surface is parameterized. We therefore use CABLE as it is a relatively sophisticated land surface model. It uses a two-leaf canopy (i.e., differentiates between shaded and sunlit leaves), positions the canopy above the ground and calculates within-canopy turbulence, temperature and humidity. It also implements coupled stomatal conductance-photosynthesis partitioning of net available energy and calculates carbon assimilation as the balance of photosynthesis and plant and soil respiratory loss. It uses a 6-layer soil and 3-layer snow model. Vegetation and soil parameters are inferred by specifying soil and vegetation types at each grid point from global maps, while surface albedo is calculated at each time step. As LULCC is imposed, associated parameters that describe the vegetation are changed according to Tables 1a and 1b. CABLE has been extensively evaluated [Abramowitz et al., 2008; Wang et al., 2011] and an earlier version was used in the Land Use Change Identification of robust impacts (LUCID) project [Pitman et al., 2009; de Noblet-Ducoudré et al., 2012]. Further, Mao et al. [2011] documents the performance of CSIRO Mk3L coupled to CABLE with a focus on terrestrial quantities. This analysis provides strong evidence that the coupled model produces a reasonable large-scale climatology.

[10] The CSIRO Mk3L climate system model is a relatively low-resolution but computationally efficient ocean-atmosphere general circulation model developed for studies of climate on centennial to millennial time scales [Phipps et al., 2011]. The atmospheric component has a horizontal resolution of 5.6° by 3.2° and 18 vertical levels, while the oceanic component has a horizontal resolution of 2.8° by 1.6° and 21 vertical levels. CO_2 concentrations at pre-industrial (280 ppmv) and doubled pre-industrial levels (560 ppmv) were applied in the experiments. For this study the atmospheric model is not coupled to the ocean. Instead, seasonally varying sea surface temperature (SST) fields corresponding to $1 \times \text{CO}_2$ and $2 \times \text{CO}_2$ levels were prescribed from climatological means derived from the last 1000 years of 7000-yearlong equilibrium simulations with the CSIRO Mk3L model.

2.2. Experimental Design

[11] To simulate the impact of LULCC and increased CO_2 we undertook two sets of experiments (Table 2). The first set of experiments were run at $1 \times \text{CO}_2$ (280 ppmv) and had either natural (FOREST1x) or perturbed (CROP1x) vegetation cover. The natural vegetation cover map represents the potential vegetation cover when there is no anthropogenic influence [Ramankutty and Foley, 1999]. The perturbed vegetation cover map, representing deforestation, was developed by modifying the natural vegetation cover based on the crop and pasture cover in year 2000 of the Land Use Harmonization data set [Hurtt et al., 2006]. This modification starts with a high-resolution ($0.5^\circ \times 0.5^\circ$) global distribution of crops and pasture. Where the crop plus pasture fraction exceeds 10% of the $0.5^\circ \times 0.5^\circ$ pixel, the whole area of the $0.5^\circ \times 0.5^\circ$ pixel is assumed to be crops and pasture. These $0.5^\circ \times 0.5^\circ$ pixels are then aggregated to the Mk3L-CABLE grid. The four most dominant vegetation

Table 1a. Parameter Values Used to Describe the Principal Vegetation Types Changed by LULCC^a

Vegetation Type	Height of Canopy (m)	V _{max} (mol m ⁻² s ⁻¹)	Leaf Area Index (Seasonally Varying)
Evergreen needleleaf forests	17.00	6.5×10^{-5}	0.42 – 3.51
Evergreen broadleaf forests	35.00	6.5×10^{-5}	3.61 – 4.68
Deciduous broadleaf forests	20.00	8.5×10^{-5}	1.08 – 5.33
Mixed forests	19.25	8.0×10^{-5}	0.49 – 4.32
Cropland	0.55	8.0×10^{-5}	0.59 – 2.11

^aChanges from these four types of forest to croplands represent more than 90% of all imposed changes. The height of the canopy is used to derive roughness length. V_{max} is a parameter used in calculating photosynthesis.

types among the high-resolution pixels within a MK3L grid are assigned to the 4 vegetation patches used by CABLE for each grid point. A map of the fraction of vegetation cover changed to cropland is shown in Figure 1. Note that the scale of croplands is geographically quite extensive but the intensity of croplands only exceeds 50% over large areas in eastern United States, Western Europe and parts of South East Asia. A second set of experiments at $2 \times \text{CO}_2$ (560 ppmv) with natural (FOREST2x) and perturbed (CROP2x) vegetation cover were also run. All simulations were run for 400 years and the daily output from the last 50 years of simulations were used in the analysis (50 years of data was used because it was sufficient for robust statistical testing). The change in the climate extremes indices due to LULCC was determined by comparing the 50-year mean of the extremes indices of CROP1x with that of FOREST1x, while the change due to increased CO₂ was determined by comparing FOREST2x with FOREST1x.

[12] We note that the perturbation imposed to represent LULCC, a change from potential vegetation to (near) current vegetation, is a relatively extreme case. However, the method by which we imposed crops and pasture cover is not as extreme as has previously been used [e.g., *Davin and de Noblet-Ducoudré*, 2010] since we retain natural forest cover within a grid square as a patch coincident with patches representing crops and pasture. However, had we used pre-industrial (i.e., ~1850) vegetation and contrasted this with current vegetation, the impacts would likely have been smaller.

Table 1b. Parameter Values for Reflectance and Transmittance Used to Describe the Principal Vegetation Types Changed by LULCC^a

Albedo Parameters	Leaf Reflectance			Leaf Transmittance		
	Visible	NIR	Thermal	Visible	NIR	Thermal
Evergreen needleleaf forests	0.08	0.35	0.01	0.05	0.25	0.01
Evergreen broadleaf forests	0.20	0.45	0.01	0.05	0.25	0.01
Deciduous broadleaf forests	0.06	0.45	0.01	0.05	0.25	0.01
Mixed forests	0.13	0.40	0.01	0.05	0.25	0.01
Cropland	0.17	0.58	0.01	0.10	0.25	0.01

^aThe leaf reflectance and transmittances are used to derive albedo at visible, near infrared (NIR) and thermal wavelengths.

Table 2. List of Experiments Performed

Experiment	Vegetation Cover	CO ₂ Concentration (ppmv)
FOREST1x	Natural vegetation cover	280
CROP1x	Forests converted to cropland	280
FOREST2x	Natural vegetation cover	560
CROP2x	Forests converted to cropland	560

2.3. Climate Extremes Indices

[13] We use an approach for assessing extremes by deriving indices from daily temperature as recommended by the CCI/CLIVAR/JCOMM Expert Team on Climate Change Detection and Indices (ETCCDI) [*Alexander et al.*, 2006]. Twelve out of the 27 climate indices recommended by the ETCCDI are used in this study (Table 3). These indices are calculated from daily maximum and minimum temperature and have been developed to assess changes in intensity, duration and frequency of extreme climate events. While the ETCCDI indices do not always represent the most extreme extremes, they do provide globally coherent measures of more moderate extremes, which can be useful for global climate change impact assessments [*Klein Tank et al.*, 2009; *Zhang et al.*, 2011]. It is important to note that ETCCDI extremes are not necessarily comparable to those estimated using extreme value theory [e.g., *Kharin et al.*, 2007]. Other indices from the ETCCDI list, which imposed regionally dependent thresholds for temperature, were not included in this global-scale analysis. We do not include changes in precipitation indices in this paper because the relatively coarse resolution of the climate model may make estimates of changes in precipitation extremes unreliable.

2.4. Assessing Local Significance

[14] Since the distribution of the indices is not necessarily Gaussian, a parametric test such as Student's t-test may be inappropriate for testing the null hypothesis that there is no statistically significant difference between the 50-year mean time series for a given index. We therefore use the two-tailed Kolmogorov-Smirnov (KS) test, a non-parametric test that makes no assumptions about the distribution of the data. This method was used by *Deo et al.* [2009] in a regional study of climate extreme indices. Grid points with statistically significant differences are shown in color (red, blue) in the bubble maps while non-significant grid points are shown as gray boxes to facilitate visualization of continental surfaces. For each of the regions of interest (globe, tropics, northern hemisphere, southern hemisphere, northern mid-latitudes and southern midlatitudes) the percentage of significant grid points (s_A) were calculated.

2.5. Assessing Field Significance

[15] The collective significance of statistical tests in a finite number of interdependent time series needs to be much larger than the nominal level [*Livezey and Chen*, 1983]. That is, if testing at a 95% confidence level, much greater than 5% of the continental surfaces should appear statistically significant to indicate field significance. As the threshold over which results may be classified as field significant differs between indices, we use bootstrapping to calculate its estimated value. Following *Kiktev et al.* [2003] and *Alexander et al.* [2006] we use a moving block re-sampling

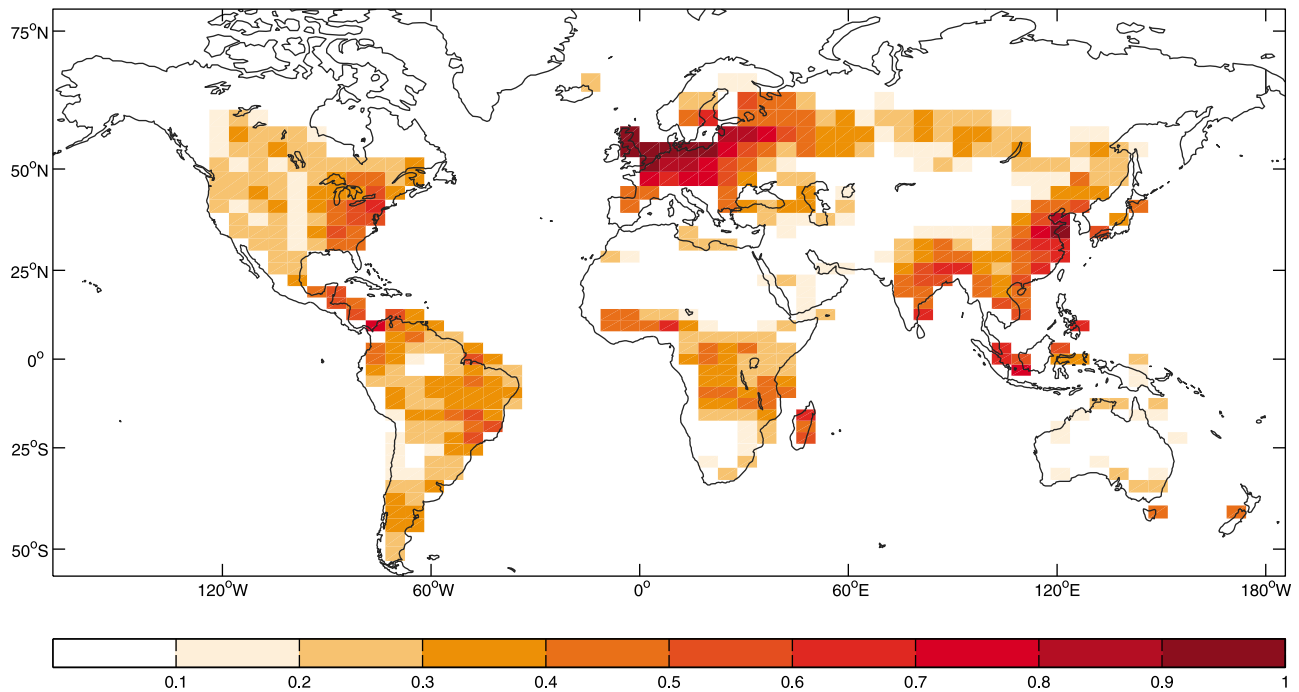


Figure 1. Fraction of vegetation cover converted from forest to cropland.

technique [Wilks, 1997] to create 1000 sets of 20-year samples by randomly taking two consecutive years of data at a time for each index and experiment. To maintain spatial dependence, all grid points were re-sampled in the same order for each experiment. For each pair of 20-year bootstrapped samples, we follow the same method used for the non-bootstrapped 50-year time series described in

section 2.4: the two-tailed KS test was applied to determine the grid points with statistically significant difference and, for each region, the percentage of significant grid points were then calculated. This resulted in 1000 percentage values for each index. The 5th percentile of these percentages, s_B , is defined as the field significance threshold level. The percentage of significant grid points of the non-bootstrapped

Table 3. A Selection of the Temperature Indices Recommended by the ETCCDI and Used in This Study^a

Index	Indicator Name	Definition	Unit
<i>Intensity</i>			
TXn	Min Tmax	Coldest seasonal daily maximum temperature	°C
TNn	Min Tmin	Coldest seasonal daily minimum temperature	°C
TXx	Max Tmax	Warmest seasonal daily maximum temperature	°C
TNx	Max Tmin	Warmest seasonal daily minimum temperature	°C
DTR	Diurnal temperature range	Mean difference between daily maximum and daily minimum temperature	°C
<i>Duration</i>			
GSL	Growing season length	Annual number of days between the first occurrence of 6 consecutive days with $T > 5^{\circ}\text{C}$ and first occurrence of consecutive 6 days with $T < 5^{\circ}\text{C}$. For the Northern Hemisphere this is calculated from 1 January to 31 December while for the Southern Hemisphere it is calculated from 1 July to 31 June.	days per year
CSDI	Cold spell duration indicator	Annual number of days with at least 6 consecutive days when $T_{\text{min}} < 10\text{th percentile}$	days per year
WSDI	Warm spell duration indicator	Annual number of days with at least 6 consecutive days when $T_{\text{max}} > 90\text{th percentile}$	days per year
<i>Frequency</i>			
TX10p	Cool days	Number of days when $T_{\text{max}} < 10\text{th percentile}$	days per season
TN10p	Cool nights	Number of days when $T_{\text{min}} < 10\text{th percentile}$	days per season
TX90p	Warm days	Number of days when $T_{\text{max}} > 90\text{th percentile}$	days per season
TN90p	Warm nights	Number of days when $T_{\text{min}} > 90\text{th percentile}$	days per season

^aPrecise definitions can be found at http://ccma.seos.uvic.ca/ETCCDI/list_27_indices.shtml. Note that ETCCDI expresses the temperature frequency indices (TX10p, TN10p, TX90p and TN90p) in percentages, but the scale used here is in number of days per 3-month season (DJF, MAM, JJA, SON).

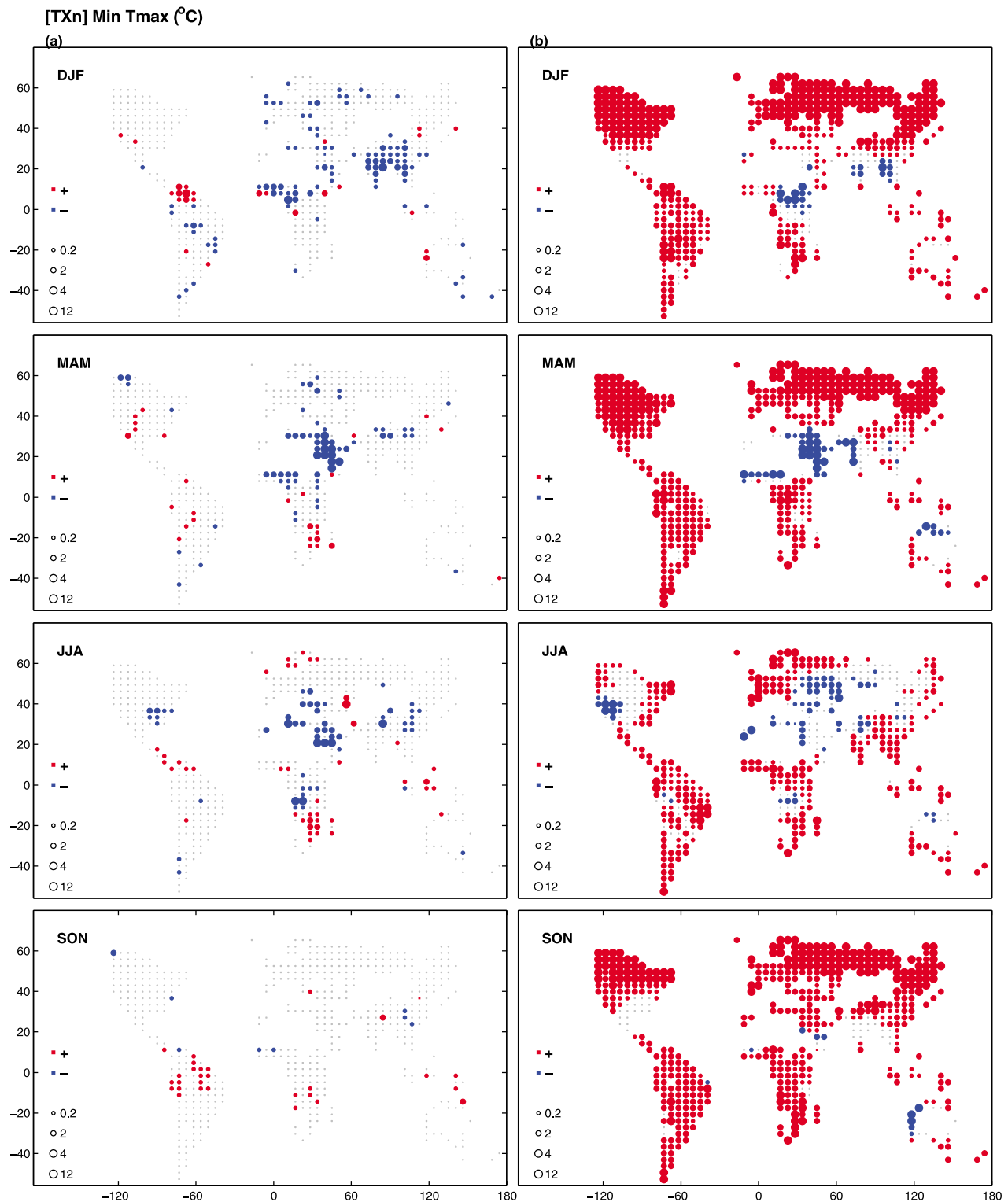


Figure 2. Difference between the 50-year mean of (a) CROP1x and FOREST1x and (b) FOREST2x and FOREST1x for coldest day-time temperature, TXn in °C. Plots are for (top to bottom) December–January–February (DJF), March–April–May (MAM), June–July–August (JJA), and September–October–November (SON). Regions with no LULCC are masked and only the grid points that are statistically significant at a 95% confidence level are shown in color (red for warming and blue for cooling). Grey dots indicate grid points that are not statistically significant. The numbers beside the legends indicate the lower bound of the range being represented by that particular circle (e.g., for Figure 2a, 0.2 represents changes ranging from 0.2 to 1.99°C; 2 = 2.0 to 3.99°C; 4 = 4.0 to 11.99°C and 12 represents other values equal to or greater than 12°C).

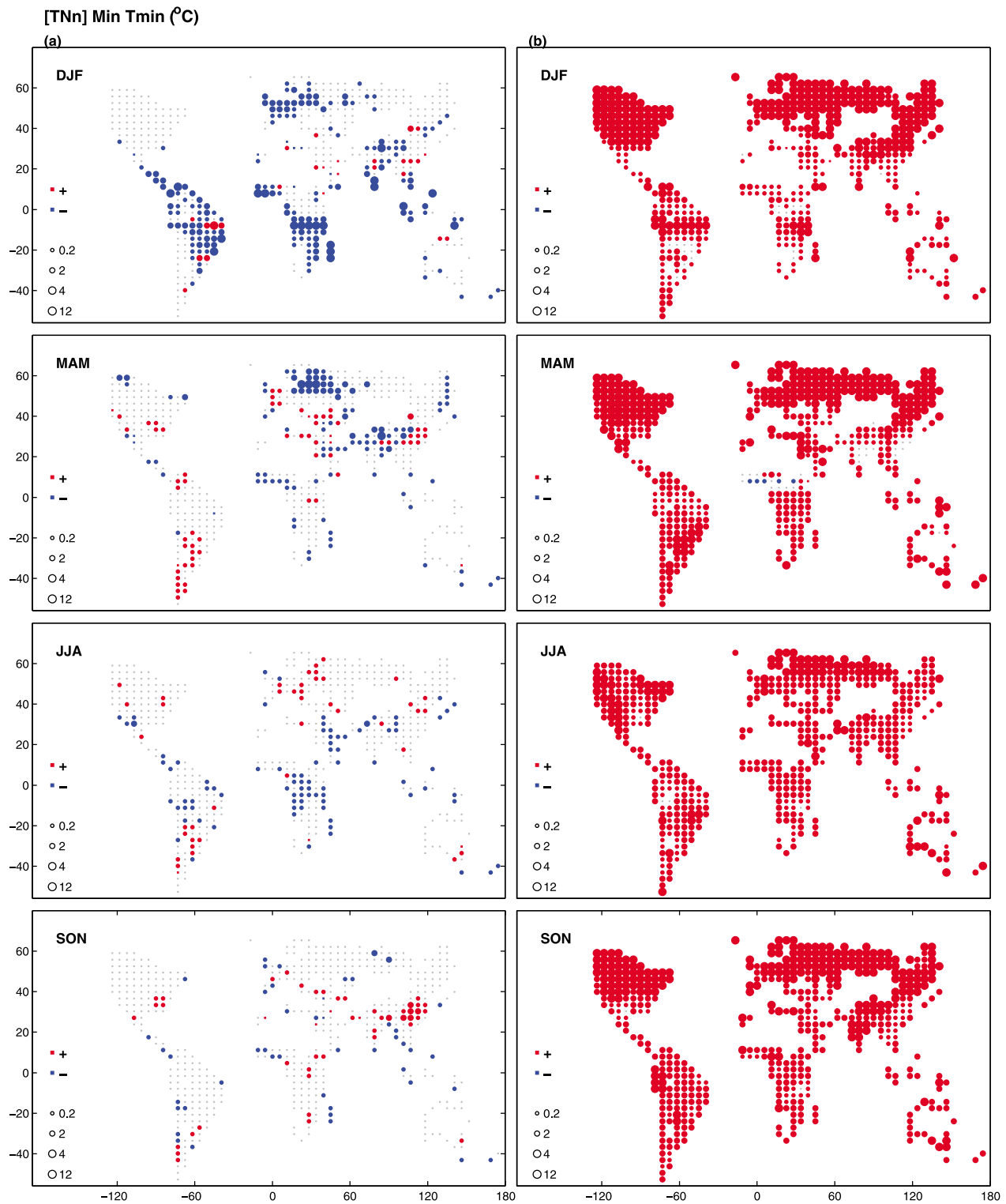


Figure 3. As in Figure 2 but for the coldest nighttime temperature, TN_n ($^{\circ}C$).

data, s_A , was then compared to this threshold. The indices are field significant if $s_B > 5$ and $s_A \geq s_B$.

3. Results

[16] We present results in the form of global bubble maps for both the impact of LULCC and the impact of $2 \times CO_2$.

The global bubble maps provide a visually efficient means to communicate those indices that are or are not significantly impacted by LULCC relative to $2 \times CO_2$. Only changes statistically significant at a 95% confidence level at a given grid box are included and we mask regions with no LULCC. Our aim here is to identify those indices strongly affected by LULCC and those near-continental scale regions where

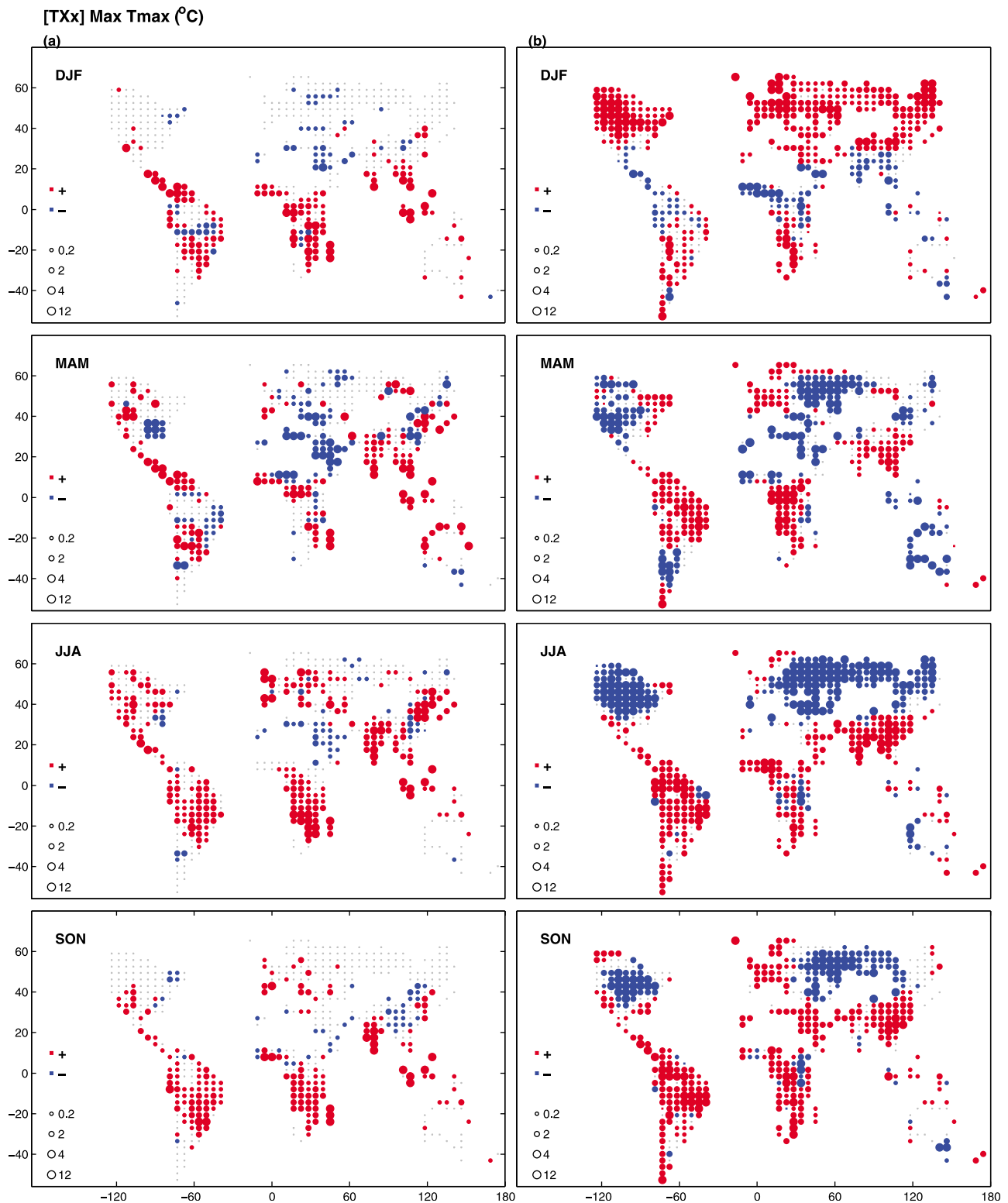


Figure 4. As in Figure 2 but for the warmest day time temperature, TXx (°C).

the temperature impact of LULCC is either of the same sign as the impact of increased CO₂, or alternatively acts to mitigate the effect of increased CO₂. To avoid any impression that temperature indices are always affected by LULCC we also include maps of indices that are negligibly perturbed.

[17] We do not discuss in detail the potential impacts of increased CO₂ on the extreme indices since this has already been well reported in the literature for both historical [e.g., Kiktev *et al.*, 2003, 2007; Christidis *et al.*, 2011] and future [e.g., Meehl *et al.*, 2007; Tebaldi *et al.*, 2006; Kharin *et al.*,

2007; Sillmann and Roeckner, 2008; Alexander and Arblaster, 2009; Russo and Sterl, 2011] time periods. We emphasize that our $2 \times \text{CO}_2$ simulations of these extremes are *indicative only* and should only be used as a reference point for the LULCC results.

3.1. Impact of LULCC on Temperature Intensity Extremes

[18] The impact of LULCC and CO_2 doubling on the coldest daily maximum temperature (TXn) is shown in Figure 2. While land areas most commonly show statistically significant warming in TXn in all seasons due to doubling CO_2 , and increases reach 12°C in the northern high latitudes in DJF, the impact of LULCC is very small (although locally statistically significant) and most commonly causes cooling of up to 2°C . This cooling in TXn is geographically isolated. The magnitude of changes due to LULCC is almost always small in comparison to CO_2 .

[19] The results for the coldest daily minimum temperature (TNn, Figure 3) are similar to those for TXn. In DJF and MAM, LULCC induces cooling in TNn of up to 4°C over parts of Eurasia (Figure 3a) but elsewhere, where significant changes occur they are almost always limited to 2°C . These are almost always substantially smaller than the impact of $2 \times \text{CO}_2$ on TNn (Figure 3b) but tend to counter $2 \times \text{CO}_2$ changes. An interesting increase in TNn occurs in SON over Asia ($1\text{--}2^\circ\text{C}$) that is additive to the increase due to $2 \times \text{CO}_2$.

[20] In many regions, LULCC causes changes in the hottest daily maximum temperature (TXx) by up to 4°C (Figure 4a). TXx increases by $2\text{--}4^\circ\text{C}$ in the tropics and sub-tropics in most seasons and by up to 2°C in the mid- and high-latitudes of the northern hemisphere in JJA. TXx cools due to LULCC by up to 2°C in the midlatitudes of the northern hemisphere in MAM. It is therefore highly geographically specific whether these changes add to, or counter, changes due to $2 \times \text{CO}_2$ (Figure 4b). In contrast to TXn and TNn, there are some regions where the magnitude of the impact of LULCC on TXx is of a similar magnitude to warming due to $2 \times \text{CO}_2$. However, note that the impact of $2 \times \text{CO}_2$ on TXx is to cool the northern hemisphere midlatitudes (MAM, JJA and SON). This is associated with a large intensification of the hydrological cycle in the climate model. This tends to increase rainfall, and thereby soil moisture and transpiration [Seneviratne et al., 2010], increasing the probability of evaporative cooling on very hot days.

[21] The general increase in TXx due to LULCC in seasons and regions with large radiation inputs is expected since the aerodynamically smoother surface post deforestation suppresses turbulent energy exchange which tends to warm the surface while the replacement of deeply rooted vegetation with shallow grasses and crops tends to limit evaporative cooling as moisture becomes limited [Teuling et al., 2010]. In contrast, a reduction in TXx over mid- and high latitudes coincident with snow cover is also anticipated since snow will mask crops more efficiently than trees leading to winter cooling [Betts, 2000]. As LULCC affects temperatures mainly in terms of albedo and the partitioning of available energy, a large impact on the hottest daily minimum temperature (TNx) would not be anticipated. Indeed, the impact of LULCC on TNx is limited to $\sim 1^\circ\text{C}$ (Figure 5a) and is negligible compared to $2 \times \text{CO}_2$ (Figure 5b).

[22] The diurnal temperature range (DTR, Figure 6) is strongly reduced (commonly by $2\text{--}4^\circ\text{C}$ but up to 12°C in JJA) by $2 \times \text{CO}_2$ over most continental areas, and is increased in the tropics in most seasons (Figure 6b) which is consistent with Vose et al. [2005]. LULCC provides a more complex pattern of changes in DTR (Figure 6a). LULCC tends to increase DTR over the northern mid- and high-latitudes in DJF and JJA, although mainly by less than 1°C , partially mitigating decreases due to $2 \times \text{CO}_2$. In the tropics and sub-tropics, LULCC tends to increase DTR in all seasons (Figure 6a); this is the same direction and magnitude of change as caused by $2 \times \text{CO}_2$ (Figure 6b). This is particularly clear in all seasons over South America where increases in DTR due to LULCC are of the same magnitude as increases due to $2 \times \text{CO}_2$. Our results therefore suggest that large-scale LULCC complicates efforts to use DTR in studies of global warming and needs to be taken into account in regions of intense landscape modification.

3.2. Impact of LULCC on Temperature Duration Extremes

[23] The growing season length (GSL, Figure 7a) is weakly affected by LULCC. GSL is locally reduced mainly by $\sim 1\text{--}5$ days per year by LULCC but is increased by a much larger amount ($10\text{--}50$ days per year) by $2 \times \text{CO}_2$. A relatively large increase in GSL (10 days per year) over China is shown in Figure 7a due to LULCC, amplifying the impact of $2 \times \text{CO}_2$ in this region.

[24] LULCC tends to increase both the cold spell durations (the number of days with at least 6 consecutive days when the minimum temperature is below the 10th percentile, CSDI, Figure 7b) and warm spell durations (the number of days with at least 6 consecutive days when the maximum temperature is above the 90th percentile, WSDI, Figure 7c). There are quite large regions where the increase in CSDI exceeds 8 days which is similar in magnitude to $2 \times \text{CO}_2$. However, while $2 \times \text{CO}_2$ systematically decreases CSDI, LULCC increases this measure thereby tending to mask the impact of $2 \times \text{CO}_2$. This contrasts with WSDI (Figure 7c) where the impact of LULCC is additive, and in many regions of similar magnitude, to the impact of $2 \times \text{CO}_2$. This leads to a complexity in the use of these indices with LULCC sometimes countering the CO_2 induced changes (CSDI) and sometimes adding to the CO_2 induced changes (WSDI).

3.3. Impact of LULCC on Temperature Frequency Extremes

[25] The impact of LULCC on the frequencies of the percentile-based temperature extremes is shown in Figures 8–11. Note that the percentiles calculated for FOREST1x are used as the threshold values when calculating the indices for the perturbed runs (CROP1x, FOREST2x), to display the differences relative to a ‘natural’ reference.

[26] The impact of LULCC on the number of days when the maximum daily temperature is below the 10th percentile (cool days, TX10p) shows a complex pattern of decreases (more than 10 days per season) principally in the tropics and sub-tropics particularly in DJF, JJA and SON (Figure 8a) but increases (mainly up to 50 days per season) in Asia (DJF), over large areas of the northern hemisphere (MAM) and over smaller areas of the northern hemisphere (JJA). The

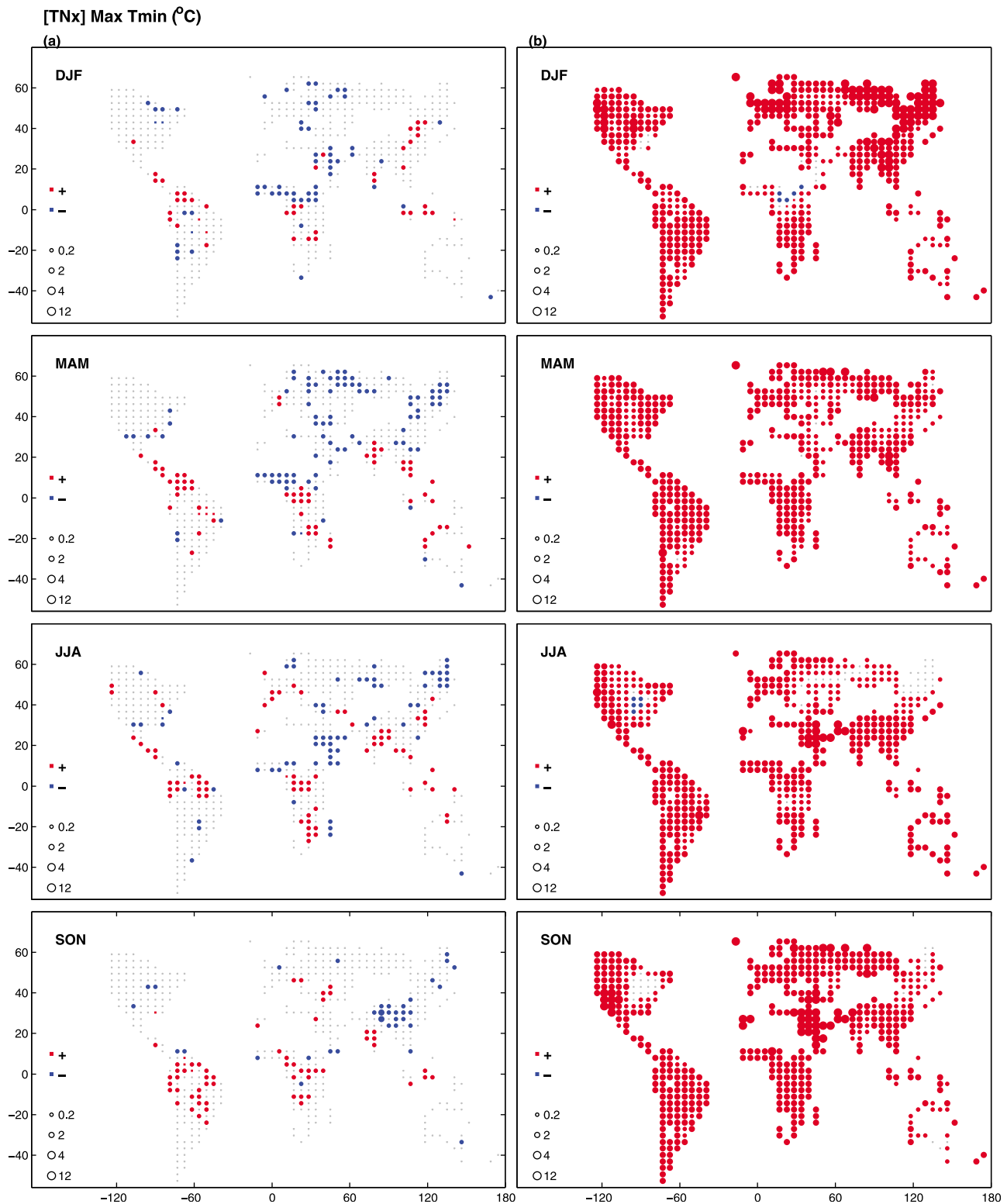


Figure 5. As in Figure 2 but for the warmest nighttime temperature, TNx (°C).

decreases in TX10p over tropical South America are particularly consistent in all seasons. The impact from $2 \times \text{CO}_2$ (Figure 8b) show increases in JJA over the northern hemisphere midlatitudes (mainly 10–50 days per season) but the dominant impacts are decreases over most continental surfaces in all seasons.

[27] Figure 9 shows the number of days when the minimum daily temperature is below the 10th percentile (cool nights, TN10p). The results for TN10p (Figure 9a) differ from TX10p (Figure 8a), including the important difference that TN10p does not change consistently over South America. In general, LULCC has a regionally statistically

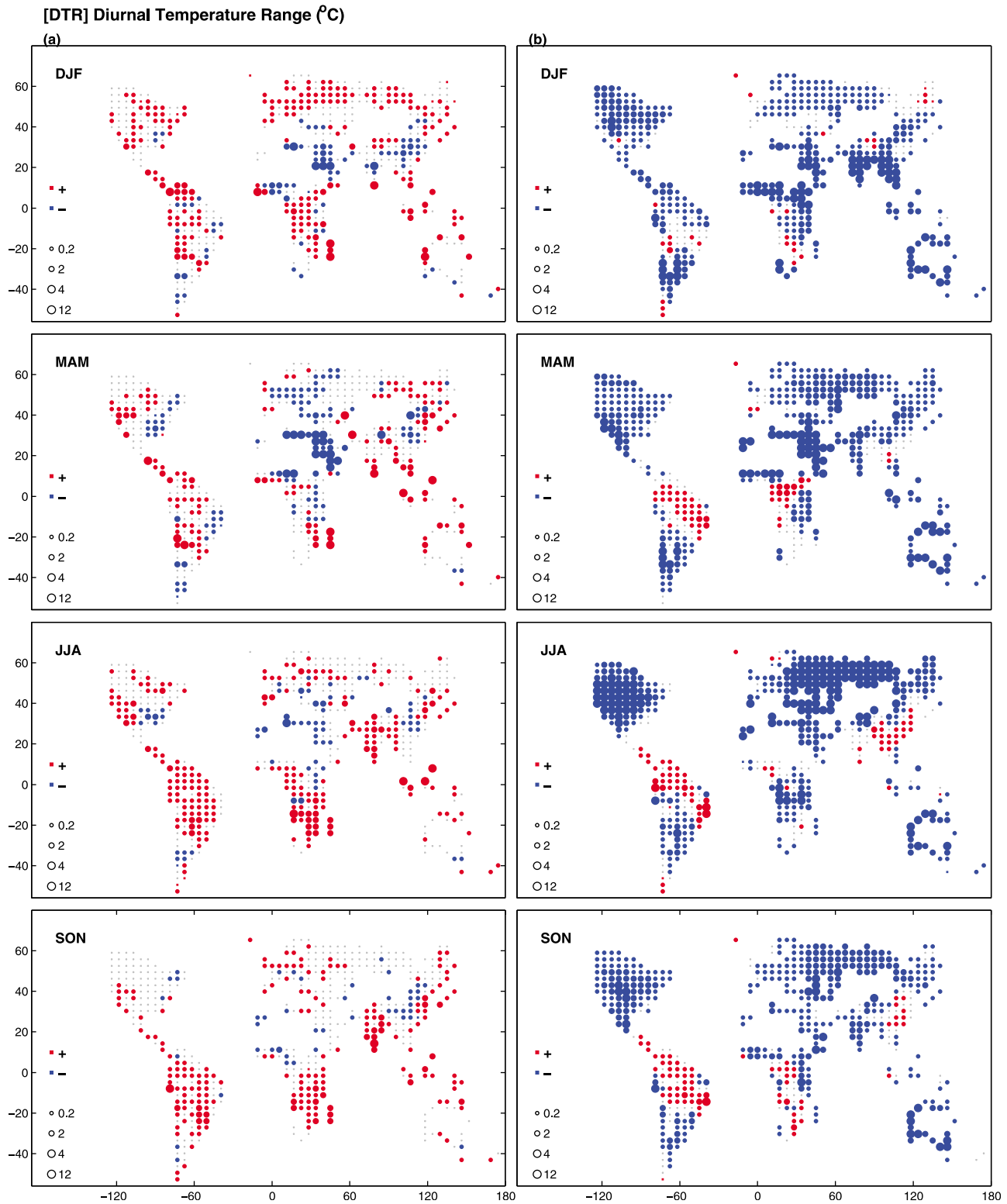


Figure 6. As in Figure 2 but for the diurnal temperature range, DTR (°C).

significant impact on TN10p, and this impact is mostly increasing this measure of extremes. This is particularly apparent in the mid- and high-latitudes of Eurasia in DJF and MAM where LULCC counters the impacts of $2 \times \text{CO}_2$. Elsewhere, relative to the impact of $2 \times \text{CO}_2$, the impacts on

TN10p are variable but are similar in magnitude to $2 \times \text{CO}_2$ in some major regions.

[28] LULCC affects the number of days when the maximum temperature exceeds the 90th percentile (warm days, TX90p) mostly by more than 10 days per season (Figure 10a).

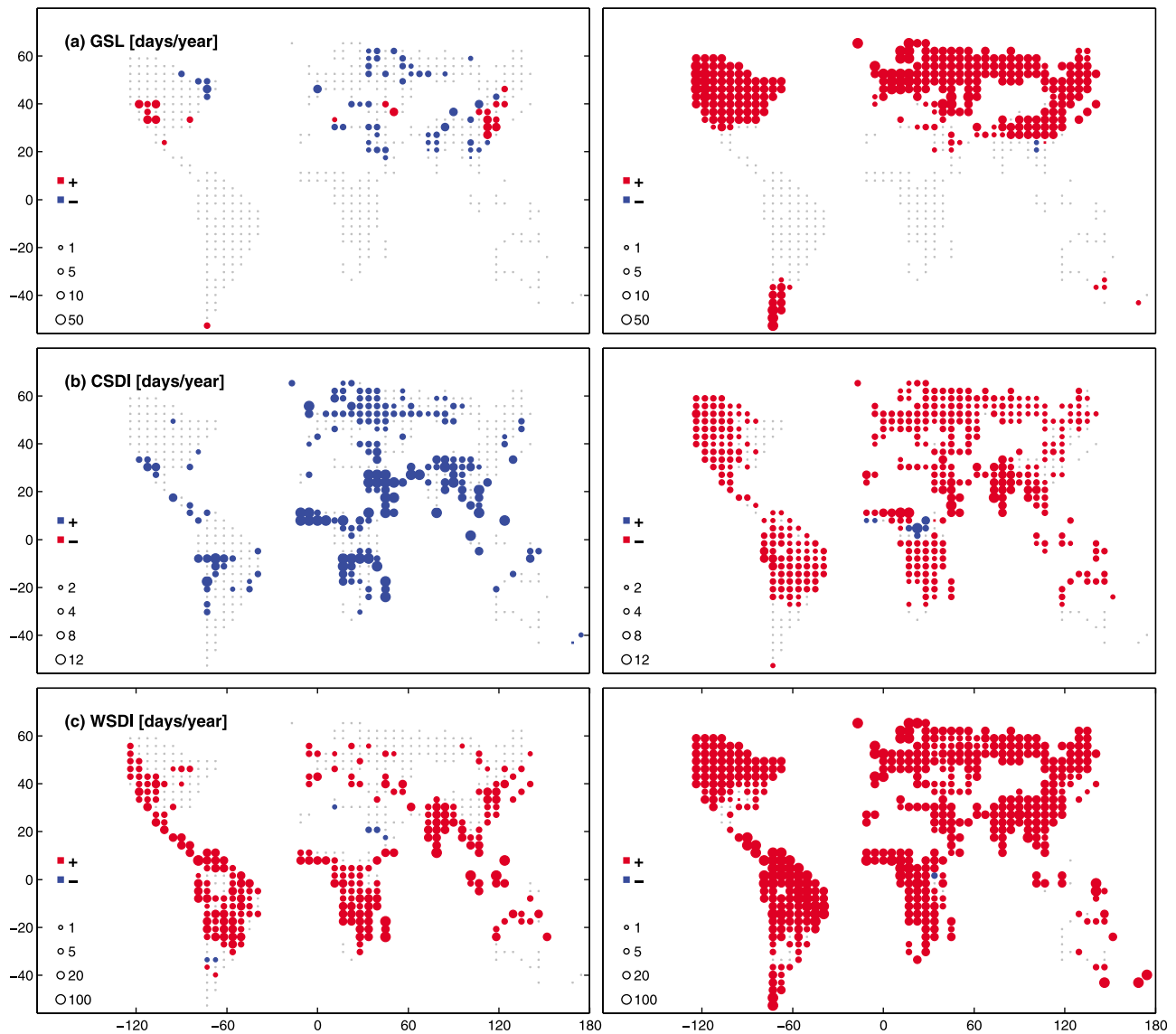


Figure 7. As in Figure 2 but for (a) growing season length, GSL; (b) cold spell duration, CSDI; and (c) warm spell duration, WSDI (all in days per year). Note that blue represents an increase in CSDI and a decrease in WSDI.

The largest and most coherent changes in TX90p occur over the tropics and sub tropics where in all seasons TX90p increases by up to 50 days per season. This is smaller than the impact of $2 \times \text{CO}_2$ (Figure 10b) but is likely additive to the increases from $2 \times \text{CO}_2$. In the mid- and high-latitudes of the northern hemisphere, LULCC tends to decrease TX90p, particularly in DJF (over Eurasia) and MAM (Eurasia and eastern U.S.) by at least 10 days per season. These decreases are of an opposite sign and of a smaller magnitude to the impacts of $2 \times \text{CO}_2$.

[29] The results for the number of days when minimum temperatures exceed the 90th percentile (warm nights TN90p, Figure 11) are smaller in terms of geographic area than shown for TX90p. While TN90p tends to increase through the tropics due to LULCC (Figure 11a) and cool in the mid- and high-latitudes of the northern hemisphere (particularly in DJF, MAM and JJA) the magnitude of

these changes is consistently small compared to the impacts of $2 \times \text{CO}_2$.

4. Discussion

[30] There is a strong consensus that LULCC affects the mean climate of regions that have been transformed by human modification of the landscape. The evidence is strong for mean temperature [Pitman *et al.*, 2009; Pielke *et al.*, 2011]. This paper examines how LULCC affects the global pattern of temperature extremes using the ETCCDI extreme climate indices derived from a set of simulations sourced from a single climate model.

[31] LULCC affects the ETCCDI temperature indices in complex ways. With regard to temperature extremes, LULCC changes the efficiency of surface exchange of water with the atmosphere [de Noblet-Ducoudré *et al.*, 2012].

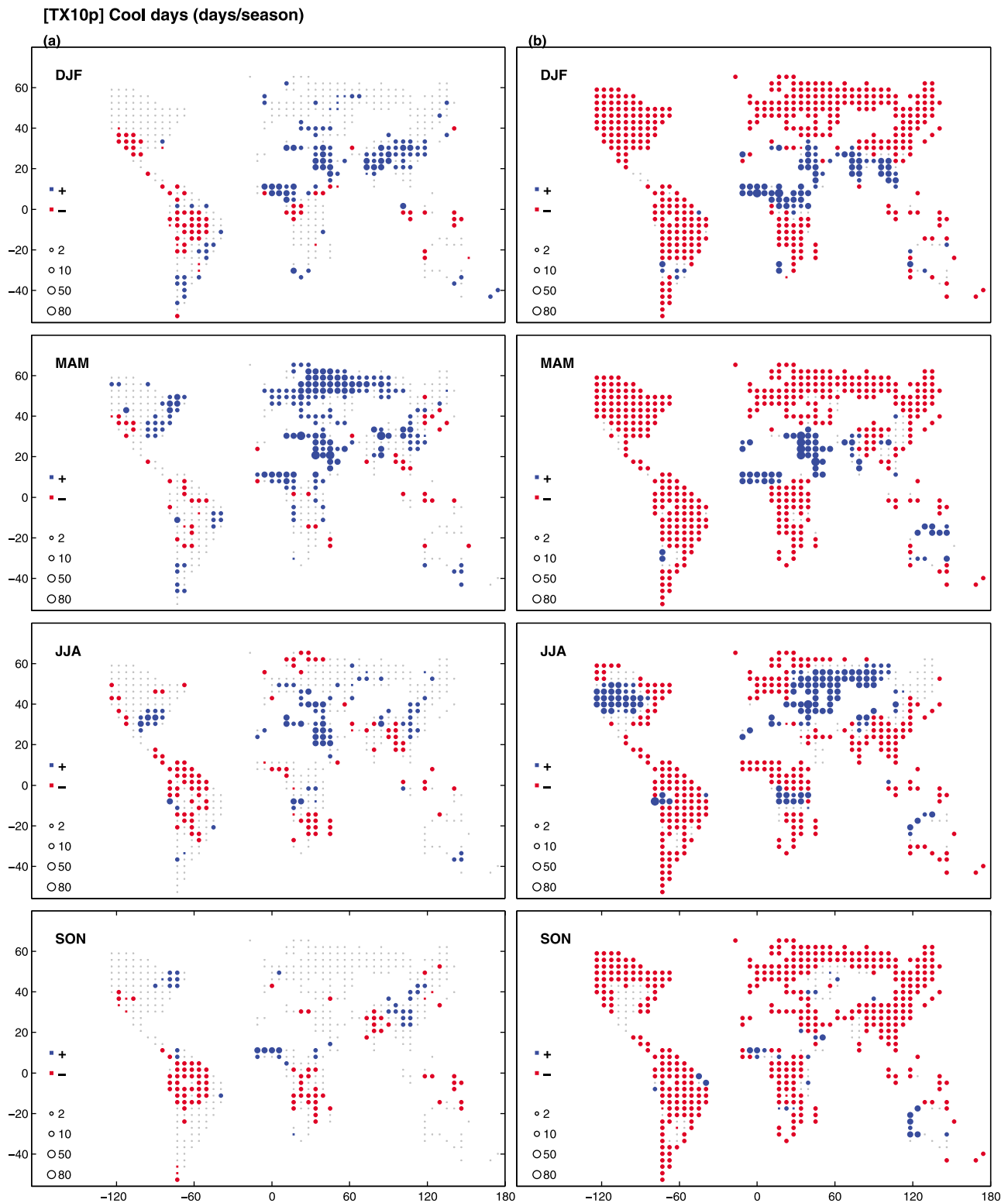


Figure 8. As in Figure 2 but for cool days, TX10p (days per season).

LULCC commonly changes a forested landscape to crops or pasture. A deeply rooted forest has a capacity to exchange moisture for longer into a dry period than a grassland which minimizes the likelihood of very high temperatures because the moisture flux cools the surface and increases atmospheric moisture and the likelihood of cloud cover [Betts

et al., 1996]. In contrast, crops and pasture limit moisture exchange earlier in a season, generally suppressing the latent heat flux and increasing the sensible heat flux. This warms the atmosphere, reduces effective moisture and reduces cloud cover, which in turn increases incident solar radiation at the surface. These mechanisms would tend to act more

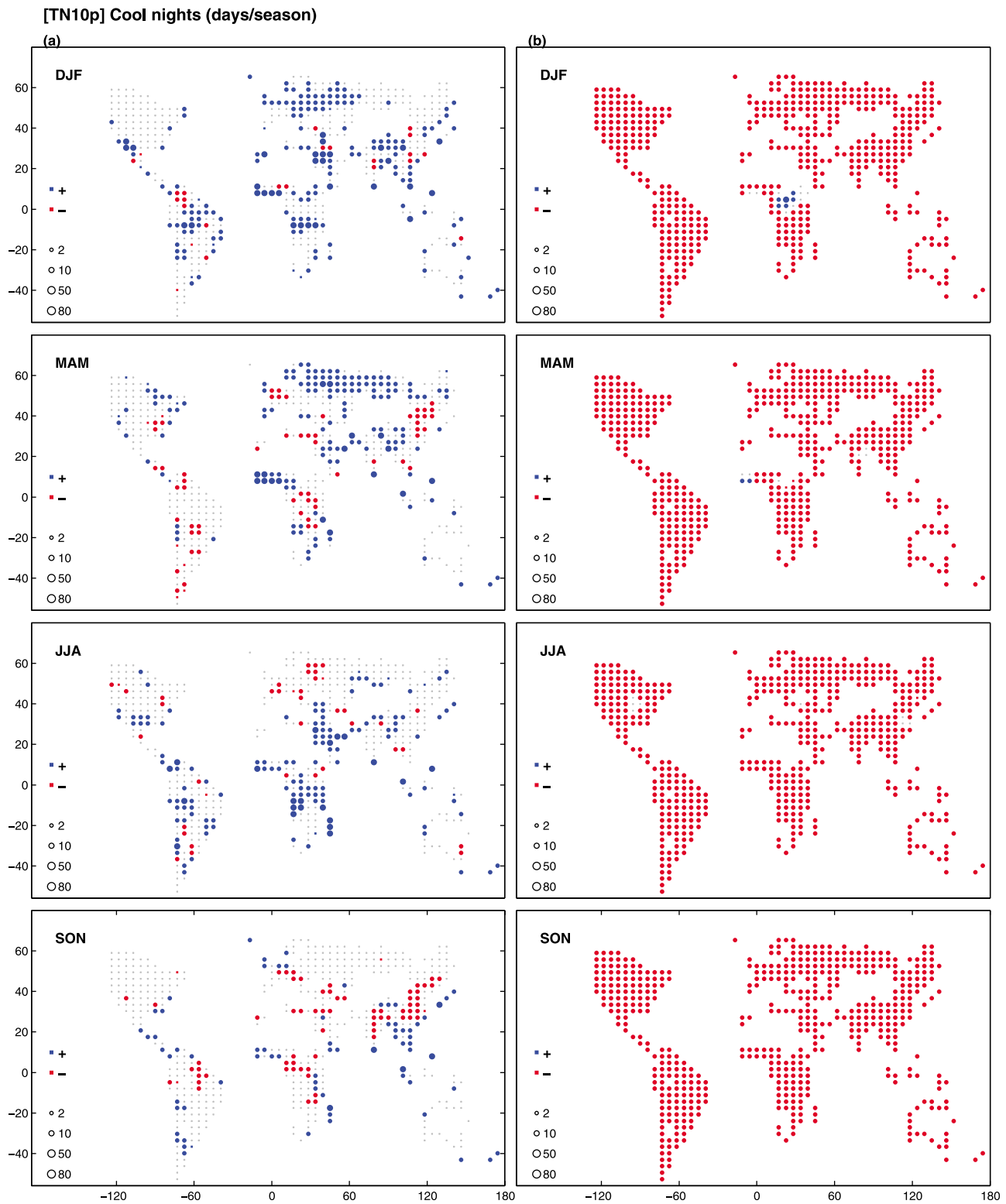


Figure 9. As in Figure 2 but for cool nights, TN10p (days per season).

directly on day-time temperatures where net radiation is strongly associated with incident solar radiation and be less significant at night where sensible and latent heat fluxes are minimal. It is not surprising therefore that the impact of LULCC is relatively large for TXx but weaker for TNx.

[32] The mean temperature impact of LULCC in our model is to warm the tropics and to cool the midlatitudes, in common with most other models [Lawrence and Chase, 2010]. If such a shift also affects the extremes, LULCC should increase the likelihood of tropical warm days (TX90p),

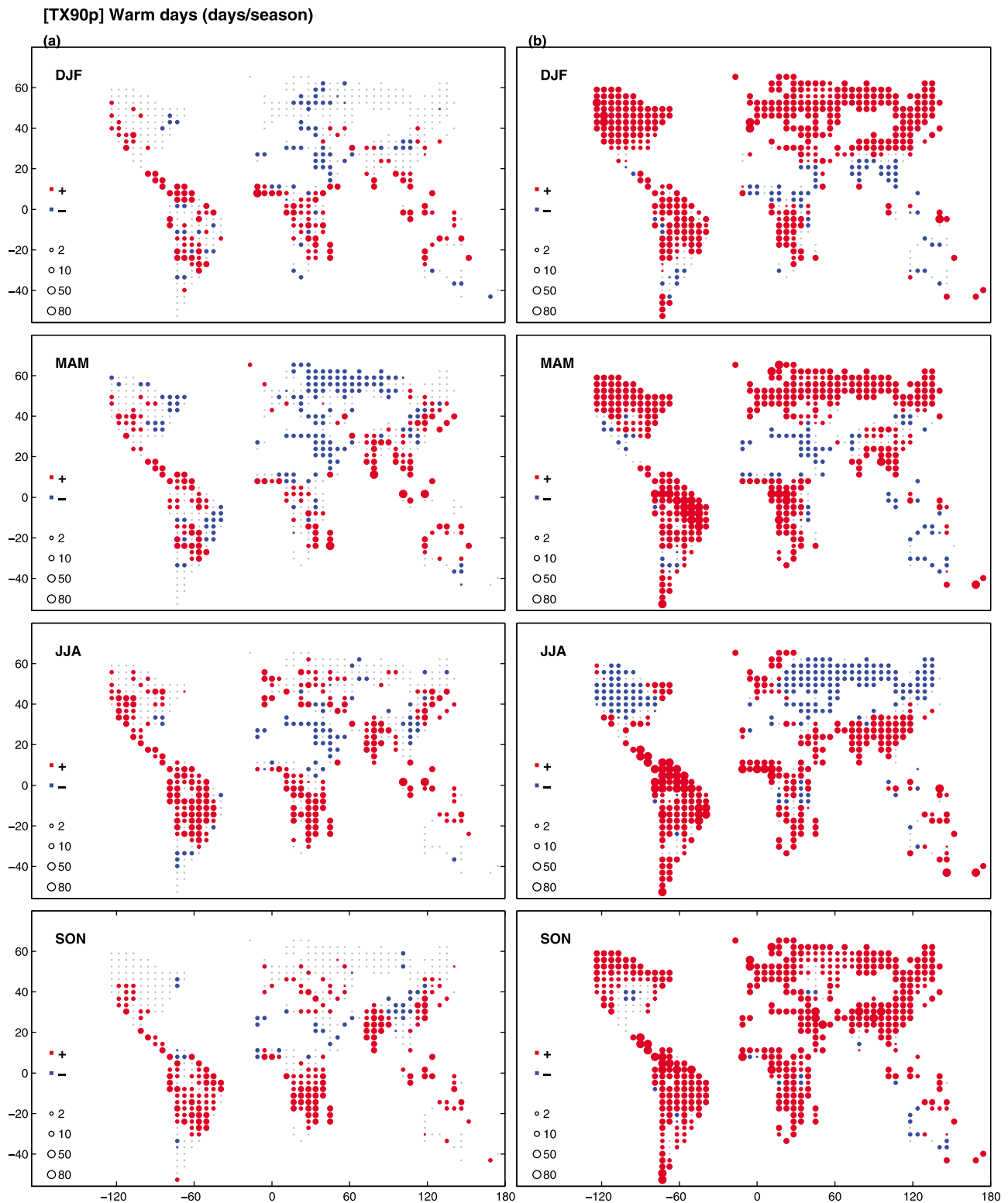


Figure 10. As in Figure 2 but for warm days, TX90p (days per season).

and tropical warm nights (TN90p) and reduce the likelihood of tropics cool days (TX10p) and tropical cool nights (TN10p). Similarly, LULCC should decrease the likelihood of midlatitude warm days and midlatitude warm nights and increase the likelihood of midlatitude cool days and nights.

Our results broadly confirm such behavior; the impact of LULCC on these temperature extremes is consistent with the mean temperature changes reported in the literature. It is noteworthy however that increases in TX10p and TN10p and decreases in TX90p and TN90p found for large areas are of

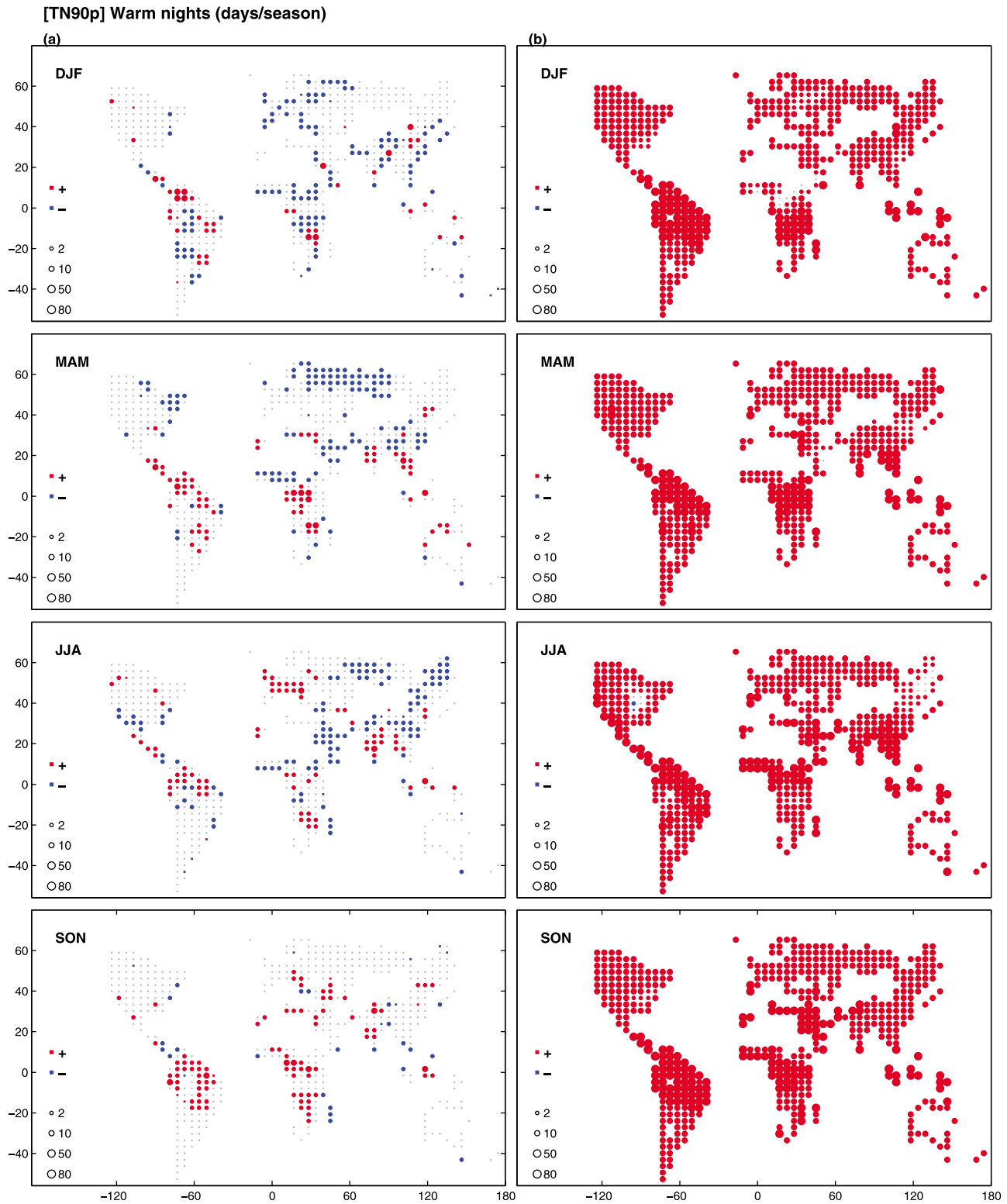


Figure 11. As in Figure 2 but for warm nights, TN90p (days per season).

the opposite sign to the impact on these indices of $2 \times \text{CO}_2$. In major regions therefore, LULCC acts to hide observable signals in these indices reducing the likelihood of detecting a change due to $2 \times \text{CO}_2$, if both forcings are considered. A similar result is found for CSDI (Figure 7b). However,

the impact of LULCC on WSDI is of the same sign and of a similar magnitude in some regions to $2 \times \text{CO}_2$ (Figure 7c) which both suggests a stronger observable signal, a stronger likelihood of a detection of a change, but a risk of misattribution of this trend to (just) elevated CO_2 . We note here that

we have also analyzed the results from simulations with perturbed vegetation cover at $2 \times \text{CO}_2$ conditions (CROP2x). The changes caused by LULCC under $2 \times \text{CO}_2$ conditions (CROP2x - FOREST2x) are, for most indices, generally similar in pattern and magnitude to the changes caused by LULCC under $1 \times \text{CO}_2$ conditions (CROP1x - FOREST1x). There are some larger differences in the LULCC signals for TN10p, TN90p (all seasons) and TNn (northern hemisphere DJF, tropics JJA) suggesting that there are nonlinearities when considering the combination of both LULCC and CO_2 forcing. However, further investigation of these effects requires a detailed regional analysis and is beyond the scope of this study.

[33] The extent of the LULCC impact on the ETCCDI temperature indices at large spatial scales, relative to the impact of $2 \times \text{CO}_2$, and the field significance of these changes is presented in Figure 12. For almost all temperature indices, $2 \times \text{CO}_2$ affects 70–100% of land grid points in all six regions in all seasons and these changes are field significant for all regions. In contrast, the LULCC impacts on the temperature indices demonstrate much more complexity. First, it is noteworthy that the impacts of LULCC are very commonly field significant for most indices for most regions and for most seasons. While the percentage of significant grid points undergoing change due to LULCC is typically half that of $2 \times \text{CO}_2$, it is only in the southern midlatitudes that changes do not appear field significant. Thus, on the broad scale, while LULCC may not trigger as large a response as $2 \times \text{CO}_2$, the response shown in Figure 12 is widespread and statistically significant. This highlights a significant challenge for those focused on the impacts of LULCC. Since the impacts of LULCC can be via an albedo feedback and/or via the change in the partitioning of available energy between sensible and latent heat, different indices are affected in different ways in different regions and in different seasons. TXx, for example, is always affected significantly in the tropics irrespective of season in a consistent way (DJF, 71%, MAM, 73%, JJA, 74%, SON 75%) while, there is a strong seasonality (DJF, 18%, MAM, 43%, JJA, 52%, SON 24%) over the northern hemisphere midlatitudes. A similar result is apparent for TX90p. In both cases, this is associated with seasonal changes in net radiation in the midlatitudes and changes in the mechanisms that link LULCC to temperature extremes.

[34] Our results have interesting implications for those analyzing the impact of anthropogenic climate change on these indices from climate model simulations that did not include LULCC. In the case of some indices, where LULCC triggers local changes of similar scale to $2 \times \text{CO}_2$, interpretation of climate model results should be undertaken very cautiously. In some regions, LULCC would suppress the impact of elevated CO_2 ; in other regions it would magnify it. This is complicated by the changes in the impact of LULCC with season. In some seasons, a given extreme index would be dominated by the change in CO_2 but in others LULCC would dominate (e.g., TNx over the northern hemisphere midlatitudes where only 13% of grid points are field significant in DJF while 21% of grid points are field significant in JJA). Assumptions that changes in many of the ETCCDI indices can be approximated by using just CO_2 changes are flawed, particularly for TXx, CSDI, WSDI, TX10p, TX90p, TN90p. However, for some regions, some indices can likely

be captured without accounting for LULCC since we provide no evidence that the inclusion of LULCC would have made a significant difference in terms of any conclusions reached at large spatial scales.

[35] Our results also have an interesting implication for detection and attribution studies. Where LULCC has a negligible impact, the detection of changes in these indices can be more safely attributed to other forcings such as CO_2 . However, where LULCC adds to other forcings, a stronger signal might be expected leading to a clearer detection of a trend, but this might also lead to a potential misattribution of that trend to non-LULCC forcing if LULCC is omitted. Similarly, where LULCC counters other forcings, a weaker net signal would tend to lead to a failure to recognize a signal because it has been masked by LULCC. This complicating feature of LULCC is seasonally and regionally dependent. While this might complicate detection and attribution studies, it also offers a way forward to refine existing methodologies. By including LULCC in future studies, a clearer and an even more robust attribution of the impact of increasing CO_2 at regional scales might be possible.

[36] We reiterate that we have been examining the impact of LULCC on the ETCCDI temperature indices at large spatial scales. LULCC has a strong and statistically significant impact at the climate model grid-scale on many of the ETCCDI temperature indices at these scales. And even where the impact of LULCC seems small compared to increasing CO_2 , in some regions it adds to the impact of elevated CO_2 and in some regions it counters this impact. There are also regions that appear to show quite large impacts due to LULCC despite the perturbation in LULCC being locally small. For example, decreases in DTR (Figure 6a), TX10p (Figure 8a) and CSDI (Figure 7b) suggest an impact from remote LULCC. There are also regional-scale impacts from LULCC coincident with intense LULCC that require further analysis and are beyond the scope of this paper due to the coarse resolution of the model used. We intend to explore the detail of the regional responses in a subsequent paper. We also intend to utilize the results from the Land Use Change Identification of robust impacts (LUCID) project [Pitman *et al.*, 2009; de Noblet-Ducoudré *et al.*, 2012]. This will enable us to determine whether results described herein are strongly limited by the climate model or the parameterization of the terrestrial surface we used. We also note that we have focused on the impacts of one major type of LULCC and omitted urbanization, irrigation and other types of land use change that could strongly affect regional climate [Pielke *et al.*, 2011].

5. Conclusions

[37] The impact of LULCC on regional-scale climate averages has been thoroughly studied and there is little doubt that strong impact on the mean temperature should be anticipated over regions of intense LULCC [Pielke *et al.*, 2011]. However, the impact of LULCC on extremes has been less well studied. In this paper we used indices recommended by the CCI/CLIVAR/JCOMM Expert Team on Climate Change Detection and Indices (ETCCDI) based on daily maximum and minimum temperature. We investigated the impact of LULCC on these indices, contrasting the large-scale impact from LULCC with a doubling of

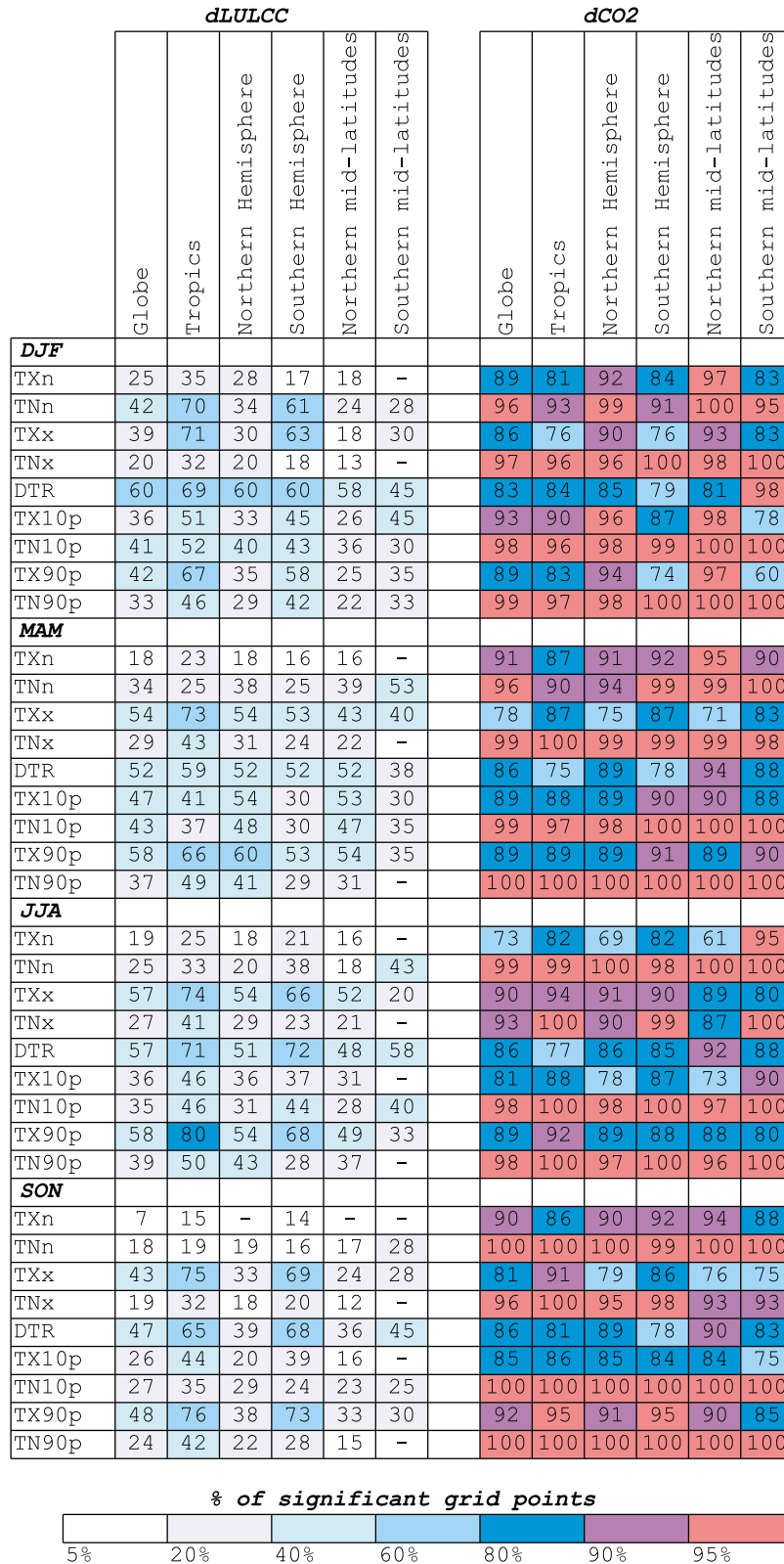


Figure 12. Seasonal field significance of the temperature extreme indices for the Globe, Tropics, Northern Hemisphere, Southern Hemisphere, Northern midlatitudes and Southern midlatitudes. Indices that are field significant are colored and shown with the percentages of statistically significant grid points in each region (s_A). Indices which are not field significant are represented by a dash.

atmospheric CO₂. Our LULCC perturbation focused on changes in vegetation from forests to crops and pasture and therefore ignores other major types of land use change such as urbanization and irrigation that could also strongly affect regional climate [Pielke *et al.*, 2011].

[38] Our results demonstrate that the impact on the ETCCDI indices of doubling CO₂ is almost always much more geographically extensive and mostly of a larger magnitude than the impact of LULCC. However, many of the temperature indices show locally strong and statistically significant responses to LULCC, such that commonly 30–50% of the continental surfaces of the tropics and northern and southern hemispheres are changed by LULCC. The scale of the impact is large enough to be field significant on seasonal timescales.

[39] We conclude that in terms of using the ETCCDI indices for climate impacts studies at large spatial scales, LULCC needs to be incorporated. In some cases, LULCC affects the ETCCDI indices in the same direction as 2 × CO₂, in other cases LULCC generates an opposing forcing. This complicates the use of climate models in regional detection and attribution studies where LULCC is omitted. However, it also provides a useful future path for detection and attribution studies since if LULCC is explicitly included, a stronger signal is likely, providing an improved capacity to attribute observed and modeled trends to known forcings.

[40] **Acknowledgments.** This research was undertaken on the NCI National Facility in Canberra, Australia, which is supported by the Australian Commonwealth Government. This work was supported in part through the ARC Centre of Excellence in Climate System Science, which is supported by the Australian Commonwealth Government. Donat and Alexander are also supported by ARC Linkage grant LP100200690. Steven Phipps provided technical support in running the Mk3L-CABLE model.

References

- Abramowitz, G., R. Leuning, M. Clark, and A. Pitman (2008), Evaluating the performance of land surface models, *J. Clim.*, *21*(21), 5468–5481, doi:10.1175/2008JCLI2378.1.
- Alexander, L. V., and J. M. Arblaster (2009), Assessing trends in observed and modelled climate extremes over Australia in relation to future projections, *Int. J. Climatol.*, *29*(3), 417–435, doi:10.1002/joc.1730.
- Alexander, L. V., *et al.* (2006), Global observed changes in daily climate extremes of temperature and precipitation, *J. Geophys. Res.*, *111*, D05109, doi:10.1029/2005JD006290.
- Bala, G., K. Caldeira, M. Wickett, T. J. Phillips, D. B. Lobell, C. Delire, and A. Mirin (2007), Combined climate and carbon-cycle effects of large-scale deforestation, *Proc. Natl. Acad. Sci. U. S. A.*, *104*(16), 6550–6555, doi:10.1073/pnas.0608998104.
- Betts, A. K., J. H. Ball, A. C. M. Beljaars, M. J. Miller, and P. A. Viterbo (1996), The land surface-atmosphere interaction: A review based on observational and global modeling perspectives, *J. Geophys. Res.*, *101*, 7209–7225, doi:10.1029/95JD02135.
- Betts, R. A. (2000), Offset of the potential carbon sink from boreal forestation by decreases in surface albedo, *Nature*, *408*(6809), 187–190, doi:10.1038/35041545.
- Bonan, G. B. (2008), Forests and climate change: Forcings, feedbacks, and the climate benefits of forests, *Science*, *320*(5882), 1444–1449, doi:10.1126/science.1155121.
- Caesar, J., L. Alexander, and R. Vose (2006), Large-scale changes in observed daily maximum and minimum temperatures: Creation and analysis of a new gridded data set, *J. Geophys. Res.*, *111*, D05101, doi:10.1029/2005JD006280.
- Canadell, J. G., and M. R. Raupach (2008), Managing forests for climate change mitigation, *Science*, *320*(5882), 1456–1457, doi:10.1126/science.1155458.
- Christidis, N., P. A. Stott, S. Brown, G. C. Hegerl, and J. Caesar (2005), Detection of changes in temperature extremes during the second half of the 20th century, *Geophys. Res. Lett.*, *32*, L20716, doi:10.1029/2005GL023885.
- Christidis, N., P. A. Stott, and S. J. Brown (2011), The role of human activity in the recent warming of extremely warm daytime temperatures, *J. Clim.*, *24*(7), 1922–1930, doi:10.1175/2011JCLI14150.1.
- Davin, E. L., and N. de Noblet-Ducoudré (2010), Climatic impact of global-scale deforestation: Radiative versus nonradiative processes, *J. Clim.*, *23*(1), 97–112, doi:10.1175/2009JCLI3102.1.
- de Noblet-Ducoudré, N., *et al.* (2012), Determining robust impacts of land-use induced land-cover changes on surface climate over North America and Eurasia; Results from the first set of LUCID experiments, *J. Clim.*, in press.
- Deo, R. C., J. I. Syktus, C. A. McAlpine, P. J. Lawrence, H. A. McGowan, and S. R. Phinn (2009), Impact of historical land cover change on daily indices of climate extremes including droughts in eastern Australia, *Geophys. Res. Lett.*, *36*, L08705, doi:10.1029/2009GL037666.
- Easterling, D. R., G. A. Meehl, C. Parmesan, S. A. Changnon, T. R. Karl, and L. O. Mearns (2000), Climate extremes: Observations, modeling, and impacts, *Science*, *289*(5487), 2068–2074, doi:10.1126/science.289.5487.2068.
- Feddema, J. J., K. W. Oleson, G. B. Bonan, L. O. Mearns, L. E. Buja, G. A. Meehl, and W. M. Washington (2005), The importance of land-cover change in simulating future climates, *Science*, *310*, 1674–1678, doi:10.1126/science.1118160.
- Findell, K. L., E. Shevliakova, P. C. D. Milly, and R. J. Stouffer (2007), Modeled impact of anthropogenic land cover change on climate, *J. Clim.*, *20*(14), 3621–3634, doi:10.1175/JCLI4185.1.
- Findell, K. L., A. J. Pitman, M. H. England, and P. J. Pegion (2009), Regional and global impacts of land cover change and sea surface temperature anomalies, *J. Clim.*, *22*(12), 3248–3269, doi:10.1175/2008JCLI2580.1.
- Forster, P., *et al.* (2007), Changes in atmospheric constituents and in radiative forcing, in *Climate Change 2007: The Physical Science Basis. Contribution of Working Group I to the Fourth Assessment Report of the Intergovernmental Panel on Climate Change*, edited by S. Solomon *et al.*, pp. 129–234, Cambridge Univ. Press, Cambridge, U. K.
- Hasler, N., D. Werth, and R. Avissar (2009), Effects of tropical deforestation on global hydroclimate: A multimodel ensemble analysis, *J. Clim.*, *22*(5), 1124–1141, doi:10.1175/2008JCLI2157.1.
- House, J. I., I. Colin Prentice, and C. Le Quéré (2002), Maximum impacts of future reforestation or deforestation on atmospheric CO₂, *Global Change Biol.*, *8*(11), 1047–1052, doi:10.1046/j.1365-2486.2002.00536.x.
- Hurt, G. C., S. Frolking, M. G. Fearon, B. Moore, E. Shevliakova, S. Malyshev, S. W. Pacala, and R. A. Houghton (2006), The underpinnings of land-use history: Three centuries of global gridded land-use transitions, wood-harvest activity, and resulting secondary lands, *Global Change Biol.*, *12*(7), 1208–1229, doi:10.1111/j.1365-2486.2006.01150.x.
- Katz, R. W., and B. G. Brown (1992), Extreme events in a changing climate: Variability is more important than averages, *Clim. Change*, *21*(3), 289–302, doi:10.1007/BF00139728.
- Khari, V. V., F. W. Zwiers, X. Zhang, and G. C. Hegerl (2007), Changes in temperature and precipitation extremes in the IPCC ensemble of global coupled model simulations, *J. Clim.*, *20*(8), 1419–1444, doi:10.1175/JCLI4066.1.
- Kiktev, D., D. M. H. Sexton, L. Alexander, and C. K. Folland (2003), Comparison of modeled and observed trends in indices of daily climate extremes, *J. Clim.*, *16*(22), 3560–3571, doi:10.1175/1520-0442(2003)016<3560:COMAOT>2.0.CO;2.
- Kiktev, D., J. Caesar, L. V. Alexander, H. Shioyama, and M. Collier (2007), Comparison of observed and multi-modeled trends in annual extremes of temperature and precipitation, *Geophys. Res. Lett.*, *34*, L10702, doi:10.1029/2007GL029539.
- Klein Tank, A. M. G., F. W. Zwiers, and X. Zhang (2009), Guidelines on analysis of extremes in a changing climate in support of informed decisions for adaptation, report, 56 pp., World Meteorol. Organ., Geneva, Switzerland.
- Lawrence, P. J., and T. N. Chase (2010), Investigating the climate impacts of global land cover change in the community climate system model, *Int. J. Climatol.*, *30*(13), 2066–2087, doi:10.1002/joc.2061.
- Levis, S. (2010), Modeling vegetation and land use in models of the Earth system, *Clim. Change*, *1*(6), 840–856, doi:10.1002/wcc.83.
- Livezey, R. E., and W. Y. Chen (1983), Statistical field significance and its determination by Monte Carlo techniques, *Mon. Weather Rev.*, *111*(1), 46–59, doi:10.1175/1520-0493(1983)111<0046:SFSASID>2.0.CO;2.
- Luber, G., and M. McGehee (2008), Climate change and extreme heat events, *Am. J. Prev. Med.*, *35*(5), 429–435, doi:10.1016/j.amepre.2008.08.021.
- Mao, J., S. J. Phipps, A. J. Pitman, Y. P. Wang, G. Abramowitz, and B. Pak (2011), The CSIRO Mk3L climate system model v1.0 coupled to the CABLE land surface scheme v1.4b: Evaluation of the control climatology, *Geosci. Model Dev. Discuss.*, *4*, 1611–1642, doi:10.5194/gmdd-4-1611-2011.

- Medvigy, D., R. L. Walko, and R. Avissar (2011), Effects of deforestation on spatiotemporal distributions of precipitation in South America, *J. Clim.*, *24*(8), 2147–2163, doi:10.1175/2010JCLI3882.1.
- Meehl, G. A., and C. Tebaldi (2004), More intense, more frequent, and longer lasting heat waves in the 21st century, *Science*, *305*(5686), 994–997, doi:10.1126/science.1098704.
- Meehl, G. A., et al. (2007), Global climate projections, in *Climate Change 2007: The Physical Science Basis. Contribution of Working Group I to the Fourth Assessment Report of the Intergovernmental Panel on Climate Change*, edited by S. Solomon et al., pp. 747–845, Cambridge Univ. Press, Cambridge, U. K.
- Phipps, S. J., L. D. Rotstayn, H. B. Gordon, J. L. Roberts, A. C. Hirst, and W. F. Budd (2011), The CSIRO Mk3L climate system model version 1.0—Part 1: Description and evaluation, *Geosci. Model Dev. Discuss.*, *4*(1), 219–287, doi:10.5194/gmdd-4-219-2011.
- Pielke, R. A., Sr., et al. (2011), Land use/land cover changes and climate: Modeling analysis and observational evidence, *Wiley Interdiscip. Rev. Clim. Change*, *2*, 828–850, doi:10.1002/wcc.144.
- Pitman, A. J. (2003), The evolution of, and revolution in, land surface schemes designed for climate models, *Int. J. Climatol.*, *23*(5), 479–510, doi:10.1002/joc.893.
- Pitman, A. J., et al. (2009), Uncertainties in climate responses to past land cover change: First results from the LUCID intercomparison study, *Geophys. Res. Lett.*, *36*, L14814, doi:10.1029/2009GL039076.
- Ramankutty, N., and J. A. Foley (1999), Estimating historical changes in global land cover: Croplands from 1700 to 1992, *Global Biogeochem. Cycles*, *13*(4), 997–1027, doi:10.1029/1999GB900046.
- Russo, S., and A. Sterl (2011), Global changes in indices describing moderate temperature extremes from the daily output of a climate model, *J. Geophys. Res.*, *116*, D03104, doi:10.1029/2010JD014727.
- Schaeffer, M., F. Selten, and J. Opsteegh (2005), Shifts of means are not a proxy for changes in extreme winter temperatures in climate projections, *Clim. Dyn.*, *25*(1), 51–63, doi:10.1007/s00382-004-0495-9.
- Seneviratne, S. I., D. Luthi, M. Litschi, and C. Schar (2006), Land-atmosphere coupling and climate change in Europe, *Nature*, *443*(7108), 205–209, doi:10.1038/nature05095.
- Seneviratne, S. I., T. Corti, E. L. Davin, M. Hirschi, E. B. Jaeger, I. Lehner, B. Orlowsky, and A. J. Teuling (2010), Investigating soil moisture-climate interactions in a changing climate: A review, *Earth Sci. Rev.*, *99*(3–4), 125–161, doi:10.1016/j.earscirev.2010.02.004.
- Sillmann, J., and E. Roeckner (2008), Indices for extreme events in projections of anthropogenic climate change, *Clim. Change*, *86*(1–2), 83–104, doi:10.1007/s10584-007-9308-6.
- Snyder, P. K. (2010), The influence of tropical deforestation on the Northern Hemisphere climate by atmospheric teleconnections, *Earth Interact.*, *14*(4), 1–34, doi:10.1175/2010EI280.1.
- Solomon, S., D. Qin, M. Manning, M. Chen, M. Marquis, K. B. Averyt, M. Tignor, and H. L. Miller (Eds.) (2007), *Climate Change 2007: The Physical Science Basis. Contribution of Working Group I to the Fourth Assessment Report of the Intergovernmental Panel on Climate Change*, 996 pp., Cambridge Univ. Press, U. K.
- Tebaldi, C., K. Hayhoe, J. Arblaster, and G. Meehl (2006), Going to the extremes, *Clim. Change*, *79*(3–4), 185–211, doi:10.1007/s10584-006-9051-4.
- Teuling, A. J., et al. (2010), Contrasting response of European forest and grassland energy exchange to heatwaves, *Nat. Geosci.*, *3*(10), 722–727, doi:10.1038/ngeo950.
- Vose, R. S., D. R. Easterling, and B. Gleason (2005), Maximum and minimum temperature trends for the globe: An update through 2004, *Geophys. Res. Lett.*, *32*, L23822, doi:10.1029/2005GL024379.
- Wang, Y. P., E. Kowalczyk, R. Leuning, G. Abramowitz, M. R. Raupach, B. Pak, E. van Gorsel, and A. Luhr (2011), Diagnosing errors in a land surface model (CABLE) in the time and frequency domains, *J. Geophys. Res.*, *116*, G01034, doi:10.1029/2010JG001385.
- Wilks, D. S. (1997), Resampling hypothesis tests for autocorrelated fields, *J. Clim.*, *10*(1), 65–82, doi:10.1175/1520-0442(1997)010<0065:RHTFAF>2.0.CO;2.
- Zhang, X., L. Alexander, G. C. Hegerl, P. Jones, A. Klein Tank, T. C. Peterson, B. Trewin, and F. W. Zwiers (2011), Indices for monitoring changes in extremes based on daily temperature and precipitation data, *Wiley Interdiscip. Rev. Clim. Change*, *2*, 851–870.
- Zhao, M., and A. J. Pitman (2002), The impact of land cover change and increasing carbon dioxide on the extreme and frequency of maximum temperature and convective precipitation, *Geophys. Res. Lett.*, *29*(6), 1078, doi:10.1029/2001GL013476.

G. Abramowitz, L. V. Alexander, F. B. Avila, M. G. Donat, and A. J. Pitman, Climate Change Research Centre, University of New South Wales, Sydney, NSW 2052, Australia. (f.avila@student.unsw.edu.au)